



Detecting the effects of rapid tectonically induced subsidence on Mayotte Island since 2018 on beach and reef morphology, and implications for coastal vulnerability to marine flooding

Matthieu Jeanson^{1,2} · Edward J. Anthony³ · Sarah Charroux^{1,2} · Aline Aubry^{1,2} · Franck Dolique⁴

Received: 3 February 2021 / Accepted: 19 November 2021 / Published online: 3 December 2021
© The Author(s), under exclusive licence to Springer-Verlag GmbH Germany, part of Springer Nature 2021

Abstract

Subsidence is a widespread phenomenon on the world's coasts. Mayotte, a coral reef-fringed archipelago in the SW Indian Ocean, experienced, in 2018 and 2019, 32 earthquakes with a recorded magnitude > 5 sourced by magmatic extraction from a deep reservoir 40–60 km east of the archipelago. This crisis resulted in island subsidence of up to 0.2 m. Profile measurements of three beaches in 2019–2021, referenced to benchmarks adjusted for subsidence, did not show any notable morphological change when compared to earlier profiles obtained in 2006/2008. This suggests that the rapid but limited subsidence has not significantly affected these systems, excluding eventual ecological repercussions that are not investigated here. Profile changes reflect seasonal variations in monsoon and trade-wind wave energy, and additionally the effect of local mild terrigenous sediment inputs. The sea-level rise caused by subsidence is, however, leading to more frequent spring high-tide flooding of some low back-beach areas and roads on the densely populated northeastern shores of the archipelago, the zone most affected by this tectonic movement. The case of Mayotte is interesting inasmuch as the subsidence caused by a distant submarine volcanic event has not been abrupt as in tectonically active areas nor continuous as in subsidence related, for instance, to glacio-isostatic readjustment, to continuous natural sediment compaction, or to anthropogenic loading. The crisis has been relatively quiescent since July 2021. Continuous monitoring will be needed to see how subsidence will eventually further affect the beach-reef flat systems of Mayotte.

Keywords Mayotte · Subsidence · Beach mobility · Coral reef · 2018–2021 Comoro Islands seismic crisis · Sea-level rise · Coastal flooding

Introduction

Many coastal regions and their beaches are subject to subsidence generated by a variety of geological and anthropogenic factors. The geological influence on beaches has been shown

to be a fundamental aspect in determining beach context and setting at the global scale, and in affecting beach morphodynamics (Anthony 2014; Gallop et al. 2020). This geological influence is also commonly manifested by tectonic activity, notably earthquakes and associated co-seismic and inter-seismic changes in land level (Wang et al. 2012) that can generate beach uplift and/or subsidence. This is notably the case of beaches situated along active tectonic margins such as in New Zealand (Little et al. 2009; Hart et al. 2020), beaches of the Columbia River littoral cell in Oregon associated with the Cascadia subduction zone (Peterson et al. 2010) and its northward extension in Alaska (Kelsey et al. 2015), the subduction coasts of Chile (Martínez et al. 2015), Sumatra and the Andaman Islands (Monecke et al. 2015), and Niigata and Kujukuri in Japan (Kuriyama and Banno 2016; Shibata et al. 2019). Subsidence affecting beaches has also been identified in areas subject to glacial-isostatic adjustments, as along the eastern seaboard of North America from Nova Scotia to Florida (Kemp et al. 2014; Forde et al.

This article is part of the Topical Collection on *Coastal and marine geology in Southern Africa: alluvial to abyssal and everything in between*

✉ Matthieu Jeanson
matthieu.jeanson@univ-mayotte.fr

¹ ESPACE-DEV, Univ Montpellier, IRD, Univ Antilles, Univ Guyane, Univ Réunion, Montpellier, France

² University Center of Mayotte CUF, Mayotte, France

³ Aix Marseille Univ, CNRS, IRD, INRA, Coll France, CEREGE, Aix-en-Provence, France

⁴ Université des Antilles, IRD and French National Museum of Natural History, UMR 207 BOREA–LabEx CORAIL, Martinique, France

2016; Fiaschi and Wdowinski 2020), often compounded by human activities. On many developed coasts, subsidence affecting beaches has also become widespread, especially along the fringes of deltas rich in fine-grained sediments and marsh vegetation that are already naturally prone to subsidence. Fine examples have been abundantly identified in the Mediterranean (e.g. Taramelli et al. 2015; Corbau et al. 2019; Amato et al. 2020; Anthony et al. 2021). Exceptionally, high temporary mud-loading over sandy beaches adjacent to high fine-grained discharge rivers can also result in short-term (seasonal) reversible subsidence (Anthony and Dolique 2006). Sources of human-induced subsidence on beaches include fluid extractions, urban development and land reclamation projects.

Mayotte, part of the coral reef-fringed Comoro archipelago in the SW Indian Ocean, experienced in 2018 and 2019 an intense seismic crisis. Over the course of a year, 32 earthquakes with a magnitude >5 occurred, with a peak of 5.9 M_w on 15th May 2018, corresponding to the largest earthquake ever felt in the region (Lemoine et al. 2020). The crisis generated some damage to infrastructure but no casualties. The origin of this earthquake activity has been attributed to magmatic extraction from a deep reservoir at a distance of 40–60 km east of Mayotte and a depth of 30–40 km that has resulted in the formation of a new $\sim 5 \text{ km}^3$ volcano about 820 m high above the ocean basement at a depth of 3500 m (Cesca et al. 2020; Lemoine et al. 2020; REVO-SIMA 2021). This volcano represents the largest active submarine eruption ever documented (Feuillet et al. 2021). The repeated earthquake activity since May 2018 has been associated with deformation of the surface of Mayotte, resulting in land subsidence. This deformation has also involved an eastward displacement of Mayotte by 21 to 25 cm (Lemoine et al. 2020; Feuillet et al. 2021). The case of Mayotte is interesting, inasmuch as the subsidence, caused by distant submarine volcanic activity, has been relatively quiescent since July 2021, and is neither the product of abrupt change as in tectonically active areas, nor of continuous readjustment as in a glacio-isostatic context, and has not been continuous as in the case of natural sediment loading and compaction.

Land subsidence along the coast can influence the elevational frame of tide and wave processes, and, thus, beach dynamics and stability. This phenomenon commonly results in greater beach exposure to storms and sea-level rise, thus generating erosion (Lithgow et al. 2019). The Mayotte crisis thus represents a rare occasion to gauge to which extent the consequences of short-lived but significant subsidence can be detected from observational data on embayed beach and adjacent reef systems. Mayotte is also subject to rising anthropogenic pressures generated by rapid population growth. These pressures, which include deforestation and catchment sediment release as well as significant impingement of housing and infrastructure on the island shores, are

also important determinants of beach and coral platform morphology and dynamics.

Physical setting

Located at about 13° S and 45° E in the north of the Mozambique Channel, Mayotte is a French overseas Department situated 300 km northwest of Madagascar and 450 km off the African continent (Fig. 1a). It is comprised of two main volcanic islands, Grande Terre and Petite Terre, with an area of 374 km^2 , representing the remnants of two underwater shield volcanoes that were active 15 Ma ago and emerged 10 Ma and 4 Ma ago respectively (Nougier et al. 1986; Audru et al. 2006; Pelletier et al. 2014). Mayotte is the oldest volcanic complex in the Comoro archipelago and, prior to the tectonic crisis of 2018, was considered to be in an advanced stage of geological development, as attested by a very low subsidence rate of 0.13 to $0.25 \text{ mm year}^{-1}$ (Colonna et al. 1996; Camoin et al. 1997, 2004) and volcanic activity on land that would have taken place less than 4000 years ago (Zinke et al. 2003). The peak elevation of the archipelago attains 660 m at Mount Bénara (Fig. 1b).

Mayotte has a 265-km-long shoreline comprising cliffs separating variably embayed pocket beaches of sand and sandy mud. The sheltered low-energy backshores of many of these beaches are characterized by mangroves (Jeanson et al. 2013). The beaches are all fringed by a reef flat ranging in width from about 50 to over 800 m and lying at an elevation, prior to the deformation crisis, of -1.8 to -2.2 m SHOM 1953 (French national geodetic reference for Mayotte), i.e., between MLWN (mean low water neaps) and MLWS (mean low water springs). This fringing reef flat is linked to a large surrounding lagoon by abrupt submarine slopes ranging from 45° to vertical cliffs several meters high. The lower beach is sometimes separated from the reef flat by a $> 0.5\text{-m}$ -deep trough visible at low tide. Mayotte has a relatively high population density of $771 \text{ inhabitants/km}^2$ and an annual demographic growth rate in the last few years that exceeds 4% per annum, resulting in strong socio-economic and ecological pressures on its volcanic islands and their beach and fringing coral reef systems.

The climate of Mayotte is humid tropical with a rainy monsoon season from October to April and a dry trade-wind season the rest of the year. The offshore wave climate is dominated by moderate waves, according to Voluntary Observing Ship (VOS) observations (sector: $12.5\text{--}13.5^\circ \text{ S}$, $44.5\text{--}45.5^\circ \text{ E}$) from 1960 to 2017 (Fig. 1f) and AVISO data from spatial altimetry (Fig. 1g). Moderate NW to NE waves are generated during the monsoon season which tends to end with relatively calm conditions that precede higher waves from S to SE (60% of observations) driven by the highly regular and sustained dry-season trade winds. Although largely sheltered by Madagascar, Mayotte can also be exposed to

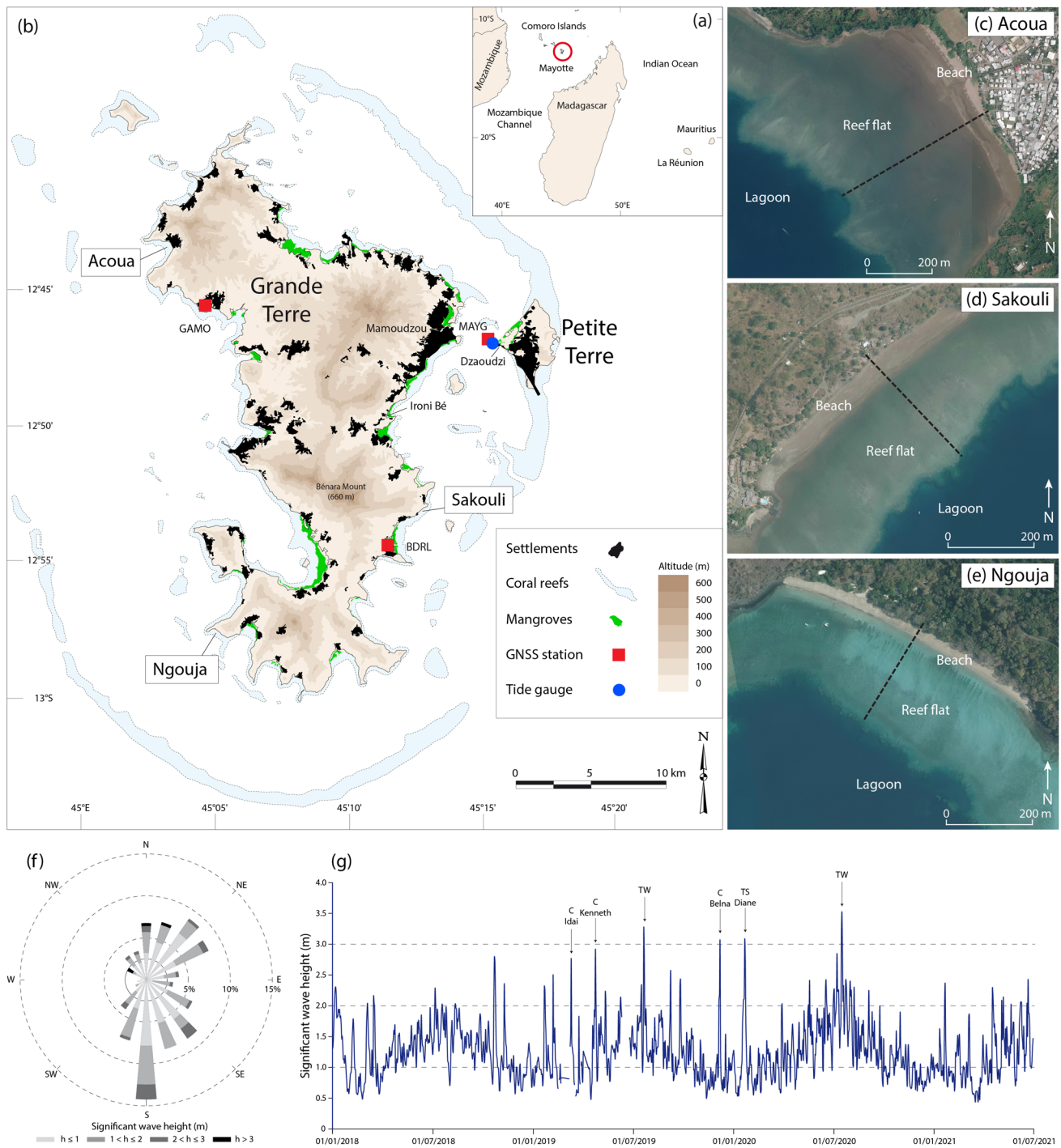


Fig. 1 **a** Location of Mayotte in the Indian Ocean. **b** simplified map of the two islands (Grande Terre and Petite Terre) and study sites; satellite pictures (Google Earth) with locations of monitored profiles of the 3 beaches: **c** Acoua, **d** Sakouli, and **e** Ngouja; **f** wave rose, 1960–2017 data from Voluntary Observing Ships; **g** deepwater sig-

nificant wave heights from January 2018 to December 2020 (TW = trade wind peak; TS = tropical storm; C = cyclone) from altimeter products processed and distributed by Aviso (<http://www.aviso.altimetry.fr/>)

tropical storms and cyclones, exclusively during the rainy season. Tides are semi-diurnal and the mean spring tidal range is about 3.2 m.

Materials and methods

Elevational changes of the substratum in Mayotte were culled from GNSS data collected by the Nevada Geodetic Laboratory

(<http://geodesy.unr.edu/NGLStationPages/stations/>) for three stations (Fig. 1). These are data processed by the NGL following the procedures by Blewitt et al. (2018). Daily-averaged sea-level data over the period 1991 to 2021 were obtained from the Dzaoudzi tidal gauge run by the REFMAR (Réseau de Références des Observations Marégraphiques) network of the French Hydrographic and Oceanographic Service (SHOM). The data comprise several gaps but the critical period of observation relevant to this study (2018–2021) shows a relatively complete record.

In order to evaluate the potential effects of the recent subsidence crisis on the beach and reef systems of Mayotte, beach profiles prior to, and following this event were compared. Unfortunately, the only available pre-subsidence profiles date back to 2006 and 2008. This shortcoming was somehow offset by a further comparison of profiles corresponding to the seismic crisis (2019, 2020, 2021) from three beach-fringing reef platform systems (Sakouli, Ngouja, Acoua) of Grande Terre (Fig. 1). The measurements covered the upper beach and the inner part of the fringing reef to offshore distances of > 500 m for Acoua, 310 m for Sakouli and 270 m for Ngouja. The surveys were carried out respectively in March 2008, November 2019, December 2020, and August 2021 at Acoua, March 2008, October 2019, October 2020, and March 2021 at Sakouli, and February 2006, December 2019, October 2020 and April 2021 at Ngouja. The earlier 2006–2008 profiles were realized using a Leica TC 407® total station, and referenced to local SHOM 1953 benchmarks. The more recent 2019, 2020, and 2021 surveys were carried out using a GNSS differential Trimble R8S® system. Given the rapid subsidence that has affected Mayotte, the benchmarks used in this study, like others in Mayotte, need to be recalibrated by the IGN (French Institut Géographique National) and SHOM. This has still not yet been done, as the final outcome of the vertical island movements is still not clear. As a result, we adjusted our 2019–2021 profiles to include the following subsidence levels (Grandin et al. 2019): 13.1 cm of downwarp for Acoua (least subsident northwestern part of Mayotte) and 18.1 cm for Sakouli (on the most subsident eastern part) and 14.4 cm for Ngouja. All surveys were carried out at low tide during comparable spring tides based on SHOM tidal coefficients. The uncertainty margins of all surveys, covering both field measurement and interpolation errors and uncertainties, was calculated respectively at ± 5 to 7 cm for x and y , and ± 5 cm for z .

Results

Elevations and tidal range

GNSS data for Mayotte show evidence of notable substrate sinking between July 2018 and July 2019 ranging from 21 to 25 cm offshore to the east and about 10 to 19 cm on various

parts of the island (Fig. 2a). Vertical movements attained about $1.5 \text{ cm month}^{-1}$ during the first 9 months of significant earthquake activity, then slowed down starting from April to May 2019 with values of the order of 0.1 to $0.3 \text{ cm month}^{-1}$. Since the end of 2020, subsidence has become negligible, dropping down virtually to the mean long-term subsidence rate evaluated at $0.19 \pm 0.06 \text{ mm year}^{-1}$ over the last ten millennia (Camoin et al. 1997). The daily-averaged sea level, the fluctuations of which reflect various tidal, seasonal, and ocean-atmosphere interaction signals, shows a clear superimposed upward shift of about 0.2 m in both low and high mean daily levels over the period of rapid subsidence between July 2018 and July 2019. The higher mean sea level persisted in July 2021 (Fig. 2b), thus indicating no reversal of subsidence.

Beach-reef platform profiles

The three profiles show a permanent break in slope between a relatively steep upper beach that forms the bulk of the mobile sediment stock and the hard reef platform more or less draped with a sediment cover that can show mobility even at the scale of the semi-diurnal tide. This break in slope has been widely observed in the numerous beaches of Mayotte by Jeanson et al. (2013) who also reported the clastic composition of these beaches. For convenience, the 2019–2021 profiles are referred to as the post-seismic profiles.

Acoua beach, northwest of the island, is 600 m long (Fig. 1b) and deeply embayed with an upper beach characterized by a permanently bermed morphology, contiguous with a moderately steep face ($\tan\beta = 0.06\text{--}0.08$) and a break in slope at about 90 m that appeared more pronounced in the post-seismic profiles (Fig. 3a). The lower beach is relatively flat and contiguous with a 400-m-wide reef flat exhibiting relatively complex bedform patterns as a result of the occurrence of muddy patches alternating with sand. Beyond this flat, the hard reef platform is devoid of sediment. The beach sediment consists of poorly sorted fine to medium sand ($D_{50} = 2.32\text{--}1.74 \Phi$), composed of weathered volcanic material and a small proportion (less than 10 %) of bioclasts. Compared to the 2008 profile, the post-seismic upper half of the beach shows a significant gain in volume, attaining a maximum elevation of 1.2 m. This sediment gain is manifested by several successive berms that are clearly visible in the 2019, 2020, and 2021 profiles. The lower half of the upper beach and the inner reef platform (between 90 and 240 m), show, overall, a decrease in elevation ranging from -0.15 to -0.35 m that integrates the adjusted profile elevation relative to the lowered (post-seismic) benchmark.

Sakouli beach, east of Mayotte, is 650 m long, mildly embayed (Fig. 1d) with a moderately steep upper beach

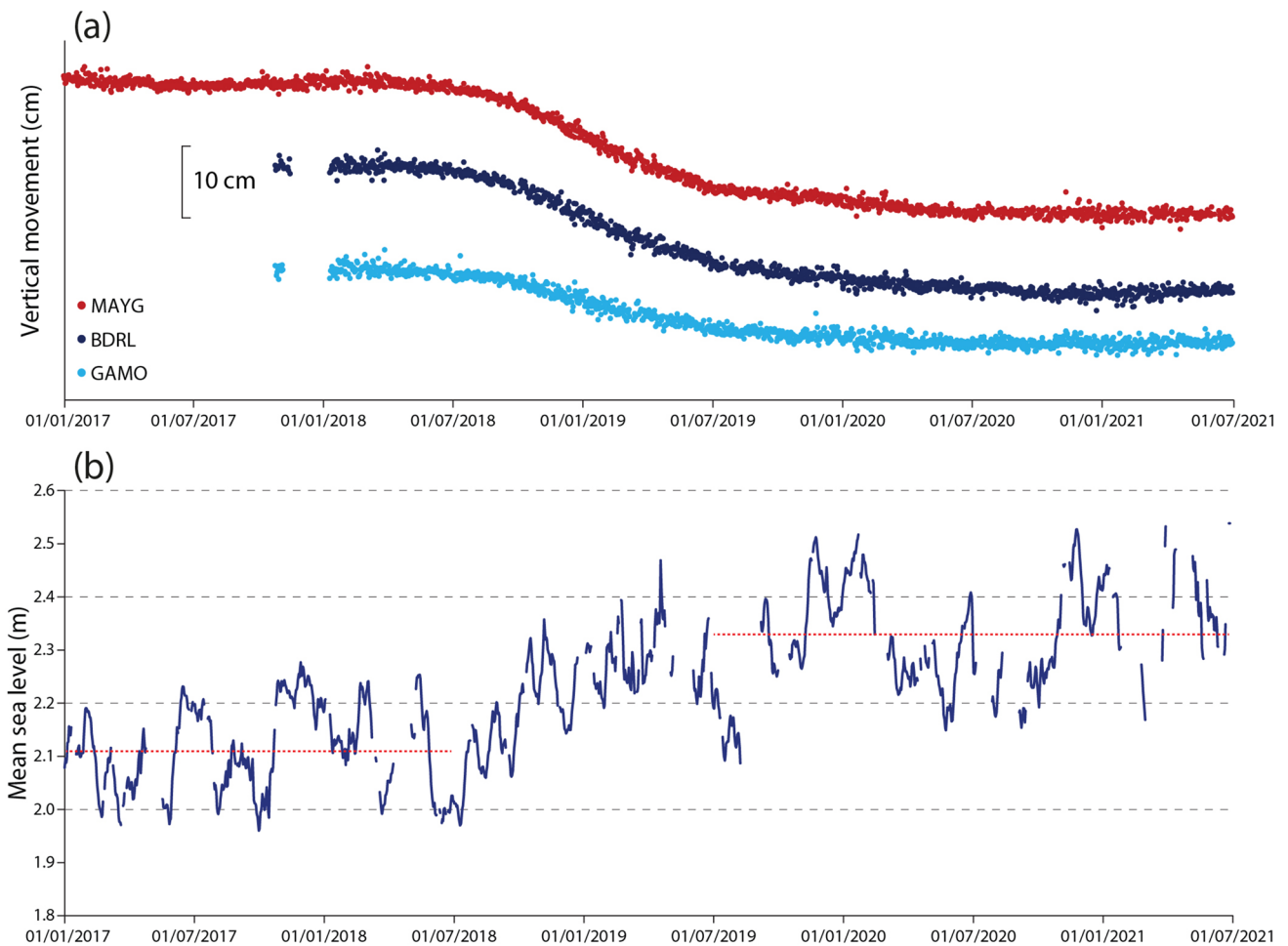


Fig. 2 **a** Vertical earth substrate displacements (cm) recorded for three GNSS stations in Mayotte (MAYG, BDRL, GAMO) between 1 January 2017 and 1 July 2021; time series were obtained from the Nevada Geodetic Laboratory with processing by Blewitt et al. (2018). The most subsided part of the archipelago is the northeast, closest to the magmatic extraction zone in the northern part of the Mozambique

Channel (Fig. 1a). **b** Mean daily sea level at the tide-gauge station of Dzaoudzi, Fig. 1b) over the same period (source: REFMAR, SHOM). The broken red lines show the distinct difference in sea level between the pre-seismic and post-seismic phases marked by the rise in level between July 2018 and July 2019

($\tan\beta = 0.06$) fringed by a 220-m-wide reef flat. The beach consists of poorly sorted medium sand ($D_{50} = 1.74\text{--}1.51 \Phi$) formed of volcanic clasts and weathered material, and less than 15% of bioclasts. Sakouli beach showed very little variation when the 2008 and post-seismic profiles are superimposed (Fig. 3b). The main change is a slight lowering (about 0.1 m) of the reef platform which shows large areas devoid of sediment alternating with mobile patches of sediment comprising coral debris, especially gravels and small boulders (max diameter 0.4 m) and sand intermixed with algae (*Turbinaria sp.*, *Padina sp.*).

Ngouja beach is moderately embayed and located on the south coast (Fig. 1e). This beach is about 650 m long, 50 to 80 m wide intertidally, has a moderately steep face ($\tan\beta$

$= 0.12$) between MHWS and MLWN, a flat low-tide beach ($\tan\beta = 0.04$) between MLWN and MLWS, and is fronted by a 200-m-wide reef flat. The sediment suite is composed of moderately to poorly sorted coarse to medium bioclastic sand ($D_{50} = 1.53\text{--}0.61 \Phi$) supplied by the fronting reef flat, and it shows a clear asymmetry towards the finer fraction which is also rich in heavy minerals comprising ilmenite, titanomagnetite, amphibolite, feldspar, and pyroxene derived from the adjacent bedrock headlands. Morphological change at Ngouja between 2006 and the post-seismic period (Fig. 3c) essentially consisted in (adjusted) lowering of the reef flat but also mild accretion of the upper beach associated with more frequently observed spring high-tide overwashing.

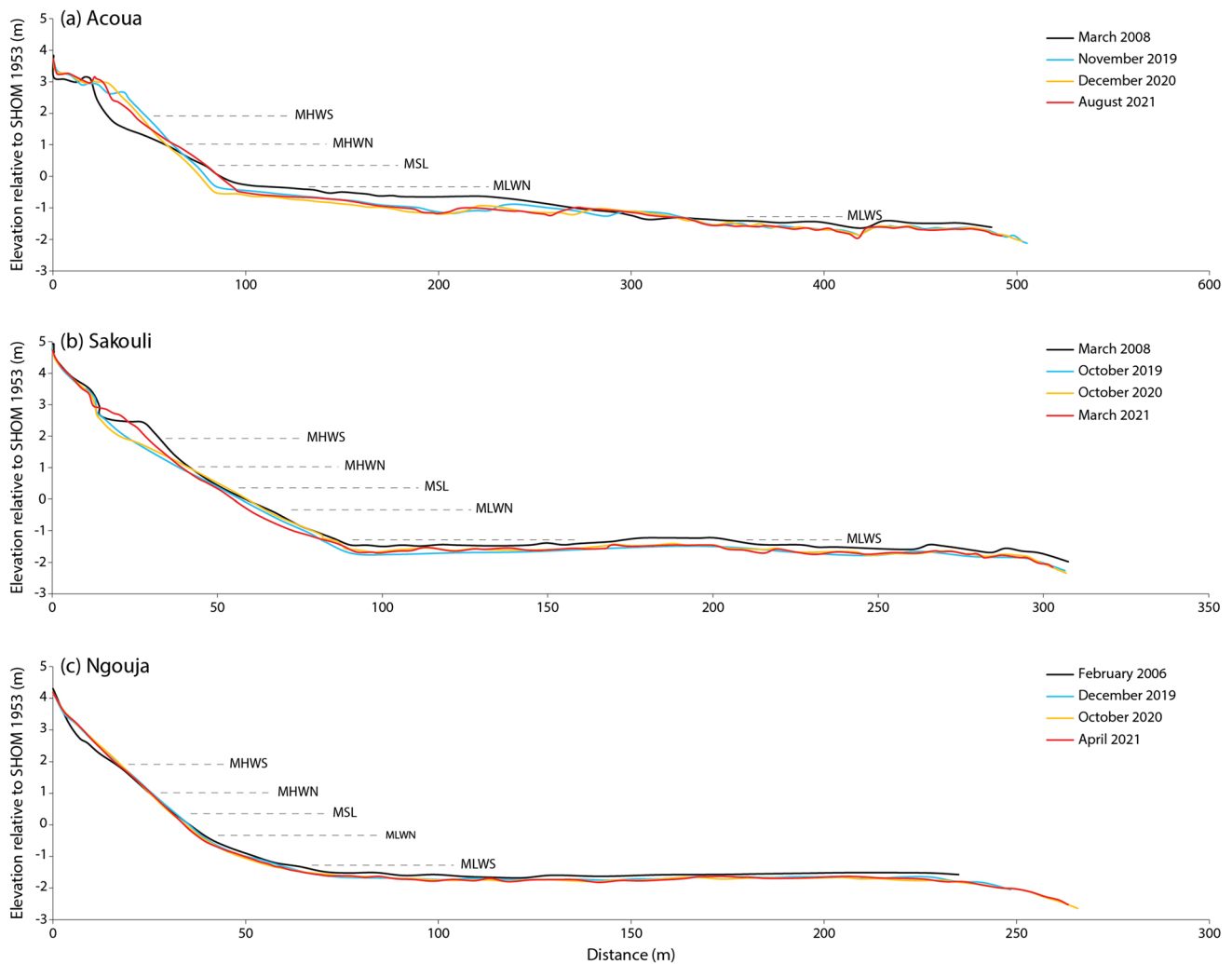


Fig. 3 Profile changes of Acoua beach/reef flat (a), Sakouli beach/reef flat (b), and Ngouja beach/reef flat (c) between 2006/2008 and the post-seismic period (2019–2021), with benchmark adjustment for island subsidence. MHWS = mean high water spring tide level;

MHWN = mean high water neap tide level; MSL = mean sea level; MLWN = mean low water neap tide level; MLWS = mean low water spring tide level

Discussion and conclusion

Subsidence affecting beaches is commonly generated by abrupt seismic movements on tectonically active coasts, by longer-term (order of millenia) isostatic readjustment on some coasts, and by modern-era anthropogenic activities on many others. All of these three sources can affect the same beaches. The last two are commonly continuous movements, although shorter-term (order of decades) anthropogenically induced subsidence affecting beaches can be reversed by appropriate actions, as in the case of the Po delta (Bezzi et al. 2021). The seismic crisis and subsidence that affected Mayotte in 2018–2019 is somewhat uncommon inasmuch as it has appeared to be an episode caused by geodynamic adjustment to a distant submarine volcanic event. The crisis generated significant short-term subsidence ranging

from 0.1 to 0.2 m, corresponding to values that should normally be cumulatively recorded over 900 years on the basis of the mean subsidence rate determined by Camoin et al. (1997) from radiometric dating (U-Th) of coral reef cores. It remains to be seen how the phase of sharp but short-lived rapid subsidence between July 2018 and July 2019 will play out in the future. The abrupt slow-down since July 2019 (Fig. 2a) goes with uncertainty regarding how this crisis will unfold. Since March 2020, subsidence measured by the GNSS stations has become negligible, and since December 2020 no coherence has been observed in the deformation signals which have become too weak and noisy to be interpretable (REVOSIMA 2021). The crisis has been relatively quiescent since July 2021 but not extinct (hundreds of tremors were recorded in July and August 2021, two with a magnitude ~ 4).

The mean daily sea level at Dzaoudzi shows a correlative stabilization at about + 0.2 m. The effects of the recent subsidence on the beach and associated coral reef platform are not obvious when the 2006/2008 topographic profiles are compared with the post-seismic profiles (Fig. 3). The potential response of beaches to sea-level rise depends on various parameters, among which are the rate of the sea-level rise, the morphological context, and sediment supply (Cooper et al. 2020). The beaches of Mayotte are relatively small, sediment-limited, but highly embayed or pocket beaches subject to marked seasonal variations driven by the monsoon and trade-wind wave regime in the western Indian Ocean (Jeanson et al. 2013, 2019). The impact of this seasonal wave regime is modulated by beach orientation and degree of embayment which play a determining role in controlling beach-surf zone sediment transport processes. The transport regime is swash-aligned in the smaller pocket beaches such as Acoua, and drift-aligned for the longer Sakouli and Ngouja beaches. Acoua beach, nested in a strongly indented bay, is dominated by seasonal cross-shore sand mobility. The upper beach morphological variations between the 2008 and post-seismic profiles could simply reflect the driving seasonal wave regime changes in this swash-aligned context. However, the Acoua embayment also receives some terrigenous sediment released from a small nearby stream. The post-seismic context, compared to the earlier 2008 profile, is one of net accretion marked by the formation of successive berms that have been progressively colonized over the 13-year period by creeping beach grass *Ipomoea pes-caprae* and the typical tree species *Terminalia catappa* and *Cocos nucifera*. The lower beach shows, however, lowering of the mobile sediment layer overlying the reef flat, and seaward of a distance of 300 m, (adjusted) lowering of the hard reef flat surface. This lowering could be a result of subsidence but the elevation change is within the error margin and may also involve the high mobility of the patchy sediment cover overlying the hard reef surface.

Sakouli and Ngouja beaches are characterized by a low bay indentation conducive to longshore sediment mobility. Like the other less embayed beaches of Mayotte, they

undergo seasonal to annual rotation (Jeanson et al. 2013). The surveyed profiles of these beaches are in the centre of each bay, a zone of sediment mobility towards the extremities of the bays, which are alternately in erosion or accretion, depending on the rotation process (Jeanson et al. 2013). As a result, the 2006/2008 profiles and the post-seismic profiles do not really capture eventual net potential sediment budget changes that can be unequivocally attributed to subsidence. The morphological changes on these two beaches are less marked than on Acoua beach.

The beaches of Mayotte and their reef-flat sediment pools seem, thus, to be adjusting well to the effects of subsidence, in the closed bay systems of Mayotte, where terrigenous sediment supply is dominant and therefore could contribute to counter-balance a slow sea-level rise through enhanced inputs. However, sediment redistribution across the profile could probably change. Visual inspection of Sakouli beach shows clear signs of erosion at high tide over the last 3 years. Parts of the upper beach are now characterized by a permanent erosional bluff with recently uprooted vegetation (Fig. 4a). At Ngouja, overwash processes not captured by the post-seismic beach profiles have also been observed in the past 2 years and are leading to increasing landward transfer of sand to unusual backshore locations (Fig. 4b) and this could ultimately impact the sediment budget of the active rotating beach. These processes are also associated with exposure of the roots of the baobab (*Adansonia digitata*) trees on the beach. The topographic variation between 2006/2008 and 2019-2021 also captures some of the lowering of the hard reef surface of both beaches, like that of Acoua, but this change may also reflect mobility of the sediment cover. Visual observations since 2018 show, however, longer submersion of these reef surfaces that is consistent with the 0.1-0.2 m sea-level rise (Fig. 2b) caused by subsidence. Acoua, like several embayed beaches of Mayotte, has a small debouching stream. This is not the case of Sakouli and Ngouja where debouching streams only function during line squalls that bring heavy temporary downpours, such that sediment inputs are essentially dependent on reworking of the bounding cliffs and reef supply. The steep catchments

Fig. 4 **a** Chronic upper-beach erosional bluff at Sakouli with fallen trees (10/2020), the visible stump is a *Casuarina equisetifolia* uprooted in September 2019 **b** Sandy overwash deposition on the backshore of Ngouja beach (04/2020)



Fig. 5 Examples showing increased coastal flooding during spring high tides in the most subsided northeastern part of the archipelago: **a** the main coastal road of Petite Terre, flooded in August 2019; **b** flooded road and interrupted traffic at Ironi Bé, Grande Terre, in November 2020. Courtesy of Mayotte's TV station *Mayotte l'ère*



of streams in Mayotte are increasingly subject to deforestation, and exposed to poor agricultural practice and rampant urbanization (Landemaine et al. 2017). But such conditions of potential enhanced future sediment availability for several beaches could also endanger coral reef growth through higher turbidity levels, exacerbating damage increasingly caused by marine litter (Mulochau et al. 2020). This could, in turn, lead to lower bioclastic sediment production and the shutting down of a supplementary sediment source for the beaches.

One important effect of subsidence is that of creating a component of “coastal squeeze”, a situation where settlements and infrastructure, immobile in nature, can be affected by sea-level rise (Lithgow et al. 2019). Mayotte is characterized by relatively steep relief, and in consequence, increasing population growth in the more topographically favorable coastal zone has led to massive mangrove down-cutting in the last few years under the pressures of illicit urban sprawl (Jeanson et al. 2014, 2019). Overall, the exposure to coastal flooding on the northeastern shores of Grande Terre and on Petite Terre (Fig. 1b), the most subsident part of the archipelago (GNSS station MAYG, Fig. 2a), but also the most populous, has increased (Fig. 5) over the last 3 years as the tidal frame has moved vertically. However, this vulnerability also reflects the effects of increasing population density and rapid infrastructure development in the narrow coastal belt.

Two final points concern the reinstallation of reliable benchmark referencing in Mayotte, and further high-resolution of coastal subsidence and elevation change. The earthquake and subsidence crisis in Mayotte has rendered current benchmarks on the island inaccurate, thus, necessitating approximate adjustments to account for the land sinking. These benchmarks will need to be readjusted by SHOM and IGN but these corrections are being deferred because the eventual cessation of this subsidence is also uncertain. It is hoped that the coastal observations presented here will be pursued in the coming years. This will need to be done under a properly recalibrated sea-level reference system. Eventually, regular in situ topographic monitoring of beach-reef morphology may need to be combined with remote sensing

approaches (e.g., Tosi et al. 2018; Amato et al. 2020; Nguyen Hao and Takewaka 2021). In the circumstances of the seismic crisis that has affected Mayotte, UAV techniques could be particularly pertinent to capture, to a higher degree of resolution than the current beach profile data, beach and reef morphology and sediment-budget changes, and especially to eventually identify any signals that may be generated by future tectonic instability and subsidence.

Acknowledgements We thank Yann Mercky for his help with the field measurements. Two reviewers provided salient suggestions for improvement.

Funding This study was supported by aid from CNRS and IRD through the project ALLIANCE (Effect of sea level rise on littoral with mangrove and coral reef). Franck Dolique received field visit support from the REEFSTOR'SAND project financed by the LabEx Corail. Sarah Charroux benefits from a thesis grant from the University Center of Mayotte and the DEAL of Mayotte.

Availability of data and materials GNSS data are publicly available at Nevada Geodetic Laboratory site, and sea-level data at Dzaoudzi publicly available at Data.shom.fr. The topographic data used in this study are available at Zenodo–Research.

References

- Amato V, Aucelli PPC, Corrado G, Di Paola G, Matano F, Pappone G, Schiattarella M (2020) Comparing geological and Persistent Scatterer Interferometry data of the Sele River coastal plain, southern Italy: Implications for recent subsidence trends. *Geomorphology* 351:106953. <https://doi.org/10.1016/j.geomorph.2019.106953>
- Anthony EJ (2014) Chapter 3 - Environmental control: geology and sediments. In: Masselink G, Gehrels R (eds) *Coastal environments and global change*. Wiley Online Library, pp 52–78. <https://doi.org/10.1002/9781119117261>
- Anthony EJ, Besset M, Zainescu F, Sabatier F (2021) Multi-decadal deltaic land-surface changes: Gauging the vulnerability of a selection of Mediterranean and Black Sea river deltas. *J Mar Sci Eng* 9:512. <https://doi.org/10.3390/jmse9050512>
- Anthony EJ, Dolique F (2006) Intertidal subsidence and collapse features on wave-exposed, drift-aligned sandy beaches subject to Amazon mud: Cayenne, French Guiana. *Earth Surf Process Landf* 31:1051–1057. <https://doi.org/10.1002/esp.1361/full>

- Audru JC, Guennoc P, Thinin I, Abellard O (2006) Bathymay: la structure sous-marine de Mayotte révélée par l'imagerie multi-faisceaux. *CR Geosci* 338:1240–1249. <https://doi.org/10.1016/j.crte.2006.07.010>
- Bezzi A, Pillon S, Popesso C, Casagrande G, Da Lio C, Martinucci D, Tosi L, Fontolan G (2021) From rapid coastal collapse to slow sedimentary recovery: The morphological ups and downs of the modern Po Delta. *Estuar Coast Shelf Sci* 260:107499. <https://doi.org/10.1016/j.ecss.2021.107499>
- Blewitt G, Hammond WC, Kreemer C (2018) Harnessing the GPS data explosion for interdisciplinary science. *EOS* 99. <https://doi.org/10.1029/2018EO104623>
- Camoin G, Collona M, Montaggioni LF, Casanova J, Faure G, Thomasin BA (1997) Holocene sea level changes and reef development in the southwestern Indian Ocean. *Coral Reefs* 16:247–259
- Camoin GF, Montaggioni LF, Braithwaite CJR (2004) Late glacial to post glacial sea levels in the Western Indian Ocean. *Mar Geol* 206:119–146. <https://doi.org/10.1016/j.margeo.2004.02.003>
- Cesca S, Letort J, Razafindrakoto HNT, Heimann S, Rivalta E, Isken MP, Nikkhoo M, Passarelli L, Petersen GM, Cotton F, Dahm T (2020) Drainage of a deep magma reservoir near Mayotte inferred from seismicity and deformation. *Nat Geosci* 13:87–93. <https://doi.org/10.1038/s41561-019-0505-5>
- Colonna M, Casanova J, Dullo WC, Camoin G (1996) Sea-Level Changes and $\delta^{18}O$ Record for the Past 34,000 yr from Mayotte Reef, Indian Ocean. *Quat Res* 46:335–339. <https://doi.org/10.1006/qres.1996.0071>
- Cooper JAG, Masselink G, Coco G et al (2020) Sandy beaches can survive sea-level rise. *Nat Clim Change* 10:993–995. <https://doi.org/10.1038/s41558-020-00934-2>
- Corbau C, Simeoni U, Zoccarato C, Mantovani G, Teatini P (2019) Coupling land use evolution and subsidence in the Po Delta, Italy: revising the past occurrence and prospecting the future management challenges. *Sci Total Environ* 654:1196–1208. <https://doi.org/10.1016/j.scitotenv.2018.11.104>
- Feuillet N, Jorry S, Crawford WC et al (2021) Birth of a large volcanic edifice offshore Mayotte via lithosphere-scale dyke intrusion. *Nat Geosci*. <https://doi.org/10.1038/s41561-021-00809-x>
- Fiaschi S, Wdowinski S (2020) Local land subsidence in Miami Beach (FL) and Norfolk (VA) and its contribution to flooding hazard in coastal communities along the U.S. Atlantic coast. *Ocean Coast Manag* 187:105078. <https://doi.org/10.1016/j.ocecoaman.2019.105078>
- Forde TC, Nedimovic MR, Gibling MR, Forbes DL (2016) Coastal evolution over the past 3000 years at Conrads Beach, Nova Scotia: the influence of local sediment supply on a paraglacial transgressive system. *Estuar Coasts* 39:363–384. <https://doi.org/10.1007/s12237-015-0016-6>
- Gallop SL, Kennedy DM, Loureiro C, Naylor LA, Muñoz-Pérez JJ, Jackson DWT, Fellowes TE (2020) Geologically controlled sandy beaches: Their geomorphology, morphodynamics and classification. *Sci Total Environ* 731:139123. <https://doi.org/10.1016/j.scitotenv.2020.139123>
- Grandin R, Beauducel F, Peltier A, Ballu V, Chanard K, Valtý P, Bonfond P, de Chabaliér JB, Shreve T, Koudogbo FN, Urdiroz A, Filatov A, Novali F, Durand P, Komorowski JC (2019) Surface deformation during the 2018–19 mayotte seismo-volcanic crisis from gnss, synthetic aperture radar and seafloor geodesy. In: *AGU Fall Meeting Abstracts*, vol. 2019, pp V52D-03
- Hart DE, Pitman SJ, Byun DS (2020) Earthquakes, Coasts... and Climate Change? Multi-hazard Opportunities, Challenges and Approaches for Coastal Cities. *J Coast Res SI* 95:819–823. <https://doi.org/10.2112/SI95-159.1>
- Jeanson M, Anthony EJ, Dolique F, Aubry A (2013) Wave characteristics and morphological variations of pocket beaches in a coral reef-lagoon setting, Mayotte Island, Indian Ocean. *Geomorphology* 182:190–209. <https://doi.org/10.1016/j.geomorph.2012.11.013>
- Jeanson M, Anthony EJ, Dolique F, Cremades C (2014) Mangrove evolution in Mayotte Island, Indian Ocean: A 60-year synopsis based on aerial photographs. *Wetlands* 34:459–468. <https://doi.org/10.1007/s13157-014-0512-7>
- Jeanson M, Dolique F, Anthony EJ, Aubry A (2019) Decadal-scale dynamics and morphological evolution of mangroves and beaches in a reef-lagoon complex, Mayotte Island. *J Coast Res SI* 88:195–208. <https://doi.org/10.2112/SI88-015.1>
- Kelsey HM, Witter RC, Engelhart SE, Briggs R, Nelson A, Haeussler P, Reide Corbett D (2015) Beach ridges as paleoseismic indicators of abrupt coastal subsidence during subduction zone earthquakes, and implications for Alaska-Aleutian subduction zone paleoseismology, southeast coast of the Kenai Peninsula, Alaska. *Quat Sci Rev* 113:147–158. <https://doi.org/10.1016/j.quascirev.2015.01.006>
- Kemp AC, Bernhardt CE, Horton BP, Kopp RE, Vane CH, Peltier WR, Hawkes AD, Donnelly JP, Parnell AC, Cahill N (2014) Late Holocene sea- and land-level change on the U.S. southeastern Atlantic coast. *Mar Geol* 357:90–100. <https://doi.org/10.1016/j.margeo.2014.07.010>
- Kuriyama Y, Banno M (2016) Shoreline change caused by the increase in wave transmission over a submerged breakwater due to sea level rise and land subsidence. *Coast Eng* 112:9–16. <https://doi.org/10.1016/j.coastaleng.2016.02.003>
- Landemaine V, Lidon B, Lopez JM, Dejean C, Bozza JL, Benard B, Parizot M, Desprats JF, Cerdan O (2017) Quantification of sediment export from two contrasted catchments of the Mayotte Island: a multi-scale observatory to fight against soil erosion and siltation of the lagoon in Mayotte Island. 19th EGU General Assembly, EGU2017, proceedings from the conference held 23-28 April, 2017 in Vienna, Austria, p 10504. 2017EGUGA..1910504L
- Lemoine A, Briole P, Bertil D, Roulle A, Fomelis M, Thinin I, Raucoules D, de Michele M, Valtý P, Hoste-Colomer R (2020) The 2018–2019 seismo-volcanic crisis east of Mayotte, Comoros islands: seismicity and ground deformation markers of an exceptional submarine eruption. *Geophys J Int* 223:22–44. <https://doi.org/10.1093/gji/ggaa273>
- Lithgow D, Luisa Martínez M, Gallego-Fernández JB, Silva R, Ramírez-Vargas DL (2019) Exploring the co-occurrence between coastal squeeze and coastal tourism in a changing climate and its consequences. *Tour Manag* 74:43–54. <https://doi.org/10.1016/j.tourman.2019.02.005>
- Little TA, Van Dissen R, Schermer E, Carne R (2009) Late Holocene surface ruptures on the southern Wairarapa fault, New Zealand: Link between earthquakes and the uplifting of beach ridges on a rocky coast. *Lithosphere* 1:4–28
- Martínez C, Rojas D, Quezada M, Quezada J, Oliva R (2015) Post-earthquake coastal evolution and recovery of an embayed beach in central-southern Chile. *Geomorphology* 250:321–333. <https://doi.org/10.1016/j.geomorph.2015.09.015>
- Monecke K, Templeton CK, Finger W et al (2015) Beach ridge patterns in West Aceh, Indonesia, and their response to large earthquakes along the northern Sunda trench. *Quat Sci Rev* 113:159–170. <https://doi.org/10.1016/j.quascirev.2014.10.014>
- Mulochau T, Lelabousse C, Séré M (2020) Estimations of densities of marine litter on the fringing reefs of Mayotte (France – South Western Indian Ocean) - impacts on coral communities. *Mar Pollut Bull* 160:111643. <https://doi.org/10.1016/j.marpolbul.2020.111643>
- Nguyen Hao Q, Takewaka S (2021) Shoreline changes along northern Ibaraki coast after the great East Japan Earthquake of 2011. *Remote Sens* 13:1399. <https://doi.org/10.3390/rs13071399>
- Nougier J, Cantagrel J, Karche J (1986) The Comores archipelago in the western Indian Ocean: volcanology, geochronology and

- geodynamic setting. *J Afr Earth Sci* 5:135–145. [https://doi.org/10.1016/0899-5362\(86\)90003-5](https://doi.org/10.1016/0899-5362(86)90003-5)
- Pelleter AA et al (2014) Melilite-bearing lavas in Mayotte (France): an insight into the mantle source below the Comores. *Lithos* 208–209:281–297. <https://doi.org/10.1016/j.lithos.2014.09.012>
- Peterson CD, Jol HM, Vanderburgh S, Phipps JB, Percy D, Gelfenbaum G (2010) Dating of late Holocene beach shoreline positions by regional correlation of coseismic retreat events in the Columbia River littoral cell, USA. *Mar Geol* 273:44–61. <https://doi.org/10.1016/j.margeo.2010.02.003>
- REVOSIMA, Volcanological and Seismological Monitoring Network of Mayotte (2021) Bulletin n°33 de l'activité sismo-volcanique à Mayotte, 26p. Report no. 2680-1205. https://www.ipgp.fr/sites/default/files/revosima_bull_n33_03092021.pdf
- Shibata R, Sato S, Yamanaka Y (2019) Study on comprehensive countermeasures for coastal erosion of Kujukuri Beach. *Coast Eng* 61:256–265. <https://doi.org/10.1080/21664250.2019.1586289>
- Taramelli A, Di Matteo L, Ciavola P, Guadagnano F, Tolomei C (2015) Temporal evolution of patterns and processes related to subsidence of the coastal area surrounding the Bevano River mouth (Northern Adriatic) – Italy. *Ocean Coast Manag* 108:74–88. <https://doi.org/10.1016/j.ocecoaman.2014.06.021>
- Tosi L, Lio CD, Teatini P, Strozzi T (2018) Land subsidence in coastal environments: Knowledge advance in the Venice coastland by TerraSAR-X PSI. *Remote Sens* 10:1191. <https://doi.org/10.3390/rs10081191>
- Wang K, Hu Y, He J (2012) Deformation cycles of subduction earthquakes in a viscoelastic earth. *Nature* 484:327–332. <https://doi.org/10.1038/nature11032>
- Zinke J, Reijmer J, Thomassin B (2003) Systems tracts sedimentology in the lagoon of Mayotte associated with the Holocene transgression. *Sediment Geol* 160:57–79. [https://doi.org/10.1016/S0037-0738\(02\)00336-6](https://doi.org/10.1016/S0037-0738(02)00336-6)

Publisher's note Springer Nature remains neutral with regard to jurisdictional claims in published maps and institutional affiliations.